European Journal of Human Genetics (2007) 15, 570–577

www.nature.com/ejhg

ARTICLE

De novo t(12;17)(p13.3;q21.3) translocation with a breakpoint near the 5′ end of the *HOXB* gene cluster in a patient with developmental delay and skeletal malformations

Ying Yue[1], Ruxandra Farcas[1], Gundula Thiel[2], Christiane Bommer[3], Bärbel Grossmann[1], Danuta Galetzka[1], Christina Kelbova[4], Peter Küpferling[4], Angelika Daser[1], Ulrich Zechner[1] and Thomas Haaf*[,1]

[1]*Institute for Human Genetics, Johannes Gutenberg University Mainz, Mainz, Germany;* [2]*Human Genetic Practice, Berlin, Germany;* [3]*Institute for Medical Genetics, Faculty of Medicine, Charite, Berlin, Germany;* [4]*Human Genetic Practice, Cottbus, Germany*

A boy with severe mental retardation, funnel chest, bell-shaped thorax, and hexadactyly of both feet was found to have a balanced *de novo* t(12;17)(p13.3;q21.3) translocation. FISH with BAC clones and long-range PCR products assessed in the human genome sequence localized the breakpoint on chromosome 17q21.3 to a 21-kb segment that lies <30 kb upstream of the *HOXB* gene cluster and immediately adjacent to the 3′ end of the *TTLL6* gene. The breakpoint on chromosome 12 occurred within telomeric hexamer repeats and, therefore, is not likely to affect gene function directly. We propose that juxtaposition of the *HOXB* cluster to a repetitive DNA domain and/or separation from required *cis*-regulatory elements gave rise to a position effect.
European Journal of Human Genetics (2007) **15,** 570–577. doi:10.1038/sj.ejhg.5201795; published online 28 February 2007

Keywords: developmental delay; disease-associated balanced chromosome rearrangement; hexadactyly; *HOXB*; position effect; skeletal malformations

Introduction

Expression of some genes, in particular of developmental control genes, is influenced by regulatory elements at some distance from the transcription and promoter regions.[1] Because many of these genes are transcription factors with tissue- and developmental stage-specific expression patterns, such position effects are difficult to study in humans. The best evidence for position effects causing human genetic disease comes from chromosomal rearrangements with breakpoints and/or microdeletions well outside the relevant genes. In a number of human developmental anomalies, including X-linked deafness,[2] holoprosencephaly,[3] campomelic dysplasia,[4] and aniridia,[5] it has been shown that the distance of the disease-causing chromosome breakpoint to the 3′ or 5′ end of the misregulated gene may be more than 1 Mb.

De novo balanced chromosomal rearrangements occur in approximately one in 2500 newborns. Because the rate of abnormal phenotypes in *de novo* translocation or inversion carriers is approximately twice as high as in random newborn populations,[6] it is plausible to assume that in about half of these cases the observed phenotype is caused by inactivation of a specific gene(s) in the breakpoint region(s). The cytogenetic and molecular characterization

*Correspondence: Professor T Haaf, Institute for Human Genetics, Mainz University, School of Medicine, Langenbeckstrasse 1, Bldg 601, Mainz 55131, Germany. Tel: +49 6131 175790; Fax: +49 6131 175690;
E-mail: haaf@humgen.klinik.uni-mainz.de
Received 7 February 2006; revised 30 December 2006; accepted 19 January 2007; published online 28 February 2007

of disease-associated balanced chromosome rearrangements has already led to the identification of numerous (>100) disease genes, showing the general usefulness of this approach.[7,8] In most published cases the pathological state was caused by disruption or deletion of a gene(s) in the breakpoint region(s). Relatively few cases exhibiting position effects have been described so far.

Here, we present a *de novo* t(12;17) translocation in a developmentally delayed boy with skeletal malformations. The breakpoint on chromosome 17q21.3 is of particular interest, because this region contains the *HOXB* gene cluster. The homeobox (*HOX*) genes belong to a family of transcription factors that play an established role in skeletal development. Specific mutations in different *HOX* genes (ie, *HOXA11*, *HOXA13*, *HOXD10*, and *HOXD13*) cause various limb malformations.[9,10] Limb and/or skeletal defects may also result from balanced translocations affecting regulatory elements around the *HOXD* gene cluster.[11,12]

Materials and methods

Classical and molecular cytogenetic techniques

Metaphase chromosome spreads of the patient and his parents were prepared from peripheral blood lymphocytes and analyzed by classical GTG banding. An EBV-transformed lymphoblastoid cell line of the patient was established for chromosome, DNA, and RNA preparations. BAC and PAC clones (Table 1) were selected from the Wellcome Trust Sanger Institute Ensembl contigs and obtained from the Resource Center Primary Database of the German Human Genome Project and ResGen (Invitrogen). Amplification of larger (10–15 kb) BAC subfragments was carried out with a series of primer pairs (Table 2) chosen from the genomic sequence of BAC RP11-463M16, as described previously.[13,14] Genomic BAC DNAs and their long-range PCR products were labeled with biotin-16-dUTP or digoxigenin-11-dUTP (Roche) by standard nick translation and FISH mapped on metaphase chromosomes.[15]

Table 1 FISH mapping results of BAC/PACs from chromosome 17q21.3

BAC/PAC probe	*Chromosomal location(Mb)*	*Relative to the 17q21.3 breakpoint*
RP11-63A1	42.4	Proximal
RP11-580I16	43.0	Proximal
RP11- 456D7	43.6	Proximal
RP11- 357H4	44.0	Proximal
CTD-2377D24	44.1	Proximal
RP11-463M16	44.2	Breakpoint spanning
RP11-501C14	44.4	Distal

Expression analyses

Cytoplasmic RNAs of lymphoblastoid cell lines from the patient and 10 normal individuals were isolated using Trizol reagent (Invitrogen) and reverse transcribed with Superscript III reverse transcriptase (Invitrogen) and random primers. *HOXB3*, *HOXB4*, *HOXB8*, *HOXB9*, *HOXB13*, *TTLL6*, *CALCOCO2*, and *SNF8* transcripts were amplified from 40 and 200 ng cDNA each, using PCR conditions and gene-specific primer pairs, as described.[16] To test biallelic *versus* monoallelic expression SNP-containing RT-PCR products were sequenced, using a Beckman CEQ 8000 Genetic Analysis System. Real-time quantitative RT-PCR analysis of *HOXB3*, *HOXB9*, *HOXB13*, *CALCOCO2*, and *SNF8* transcripts was performed with predesigned and optimized TaqMan Gene Expression Assays (Applied Biosystems) on an Applied Biosystems 7500 Real-Time PCR System according to the manufacturer's instructions. Relative quantification was carried out with the delta-delta-CT method, using *GAPDH* as endogenous control.

Results

Clinical presentation

The boy was born in the 37th gestational week with a weight of 2520 g, a length of 51 cm, and microcephaly. He had low-set and posteriorly rotated ears, macrostomy, coarse facial features, postaxial hexadactyly of the feet, clinodactyly of the fingers, and bilateral inguinal hernia. He also had a funnel chest and a bell-shaped thorax (Figure 1). Owing to an intracerebral hemorrhage he developed a posthemorrhagic hydrocephalus that required insertion of a vetriculoperitoneal shunt. At 5 years of age his gross and fine motor skills, his mental development, and his language skills were all markedly delayed.

Breakpoint mapping

G-banding analysis (at a 500 band level) of the patient revealed an apparently balanced reciprocal translocation between the short-arm tip of chromosome 12 and the

Table 2 Long-range PCR fragments of the breakpoint-spanning BAC RP11-463M16

Fragment	*Forward primer (5′–3′)*	*Reverse primer (5′–3′)*	*Position in clone (bp)*
463M16A	ggt cac atg att cag gct gc	gcg aag gtc tca tgg aat ga	1571–13 640
463M16G	gag aca cca aga agc ttc ag	gat atc cga gct act cac ca	51 021–64 260
463M16C	act cat gga tag ctc aca gg	tgg tga gct aag gag aca ca	80 861–92 280
463M16F	tag gag ctg aat gag cat gc	ttg ctg gac aag gct gta ca	169 811–181 200

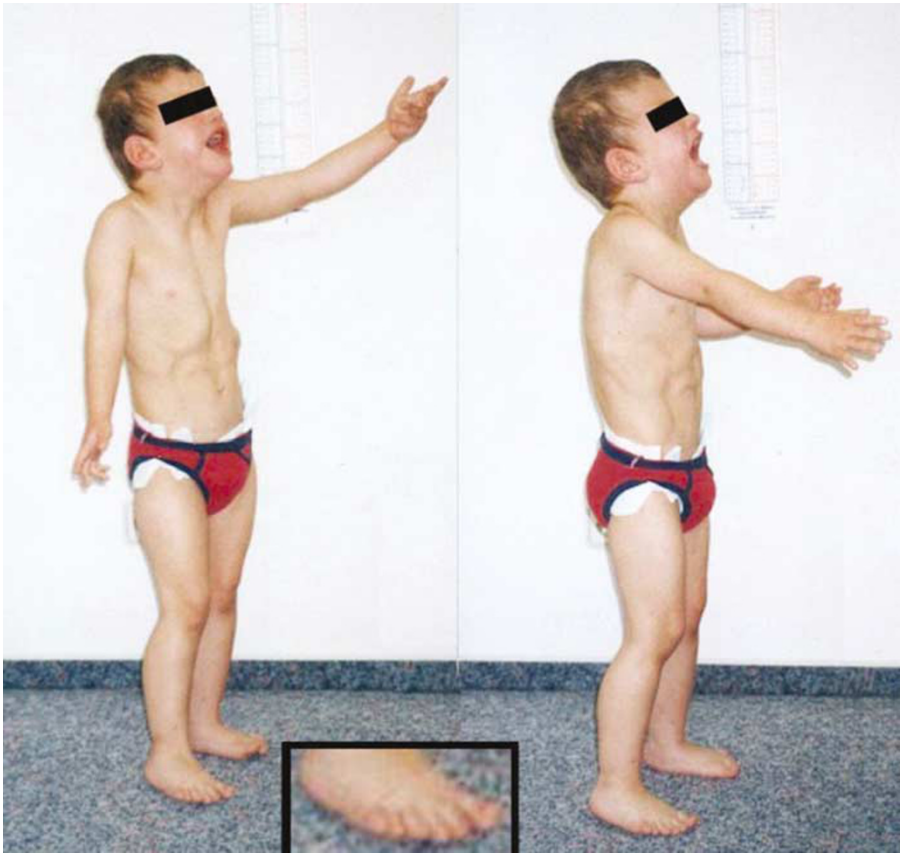

Figure 1 Patient with *de novo* t(12;17)(p13.3;q21.3) at the age of 5 years. Note the funnel chest and hexadactyly (inset) of both feet.

proximal long arm of chromosome 17 (Figure 2a), 46,XY,t(12;17)(p13.3;q21.3). The parental karyotypes were normal.

A 12p subtelomeric probe (8M16/SP6, Vysis) hybridized to the normal and derivative chromosome 12 of the patient (Figure 2b), whereas a 17q subtelomeric probe (D17S928, Vysis) produced signals on the der(12) and the normal 17 (data not shown). A telomeric hexamer repeat probe (Q-Biogene) hybridized to both ends and an interstitial site corresponding to the 12p13.3 breakpoint on the der(12) and to both ends of the der(17), as well as to other chromosome ends (Figure 2c). This implies that the 12p breakpoint occurred within the TTAGGG repetitive region and only telomeric repeats were translocated onto the der(17). On the other hand, it is possible that the distal long arm of chromosome 17 was added to an intact chromosome 12 and the chromosome 17 breakpoint was repaired by the addition of telomeric hexamer repeats. Telomeric sequences can be inserted at chromosomal breaks either directly by the telomerase enzyme or by non-homologous end-joining of a blunt-ended double-stranded telomeric DNA fragment.[17,18] However, regardless of whether the der(12) is the result of a true translocation exchange or capture of telomeric sequences, gene content and order of the 12p13.3 region remained undisturbed. Thus, we focussed our positional cloning efforts on the der(17), looking for loss, disruption, or otherwise inactivation of a dosage-sensitive gene(s) in the breakpoint region.

To narrow down the critical region, BAC and PAC clones from chromosome 17q21.3 were cohybridized with chromosome 12qter and 17pter identification probes to the patient's metaphase spreads and mapped relative to the breakpoint (Table 1). A breakpoint-containing BAC contig (Figure 2g) was assembled from the database. PAC CTD-2377D24 (Figure 2g, blue bar) hybridized to both the normal 17 and the der(17) (Figure 2d, red probes indicated by arrows) and, thus, appears to lie proximal to the breakpoint. BAC RP11-463M16 (Figure 2g, red bar), which partially (50 kb) overlaps CTD-2377D24, produced FISH signals on the normal 17 and on both derivative chromosomes (Figure 2e, red probes indicated by arrows), indicative of a breakpoint-spanning clone.

Four long-range PCR products of BAC RP11-463M16 were generated for higher-resolution mapping (Figure 2g, orange bars; Table 2). As expected, fragment 463M16A, which is also contained in PAC CTD-2377D24, hybridized to the normal 17 and the der(17), proximal to the breakpoint. Fragments 463M16G (Figure 2f, red probes

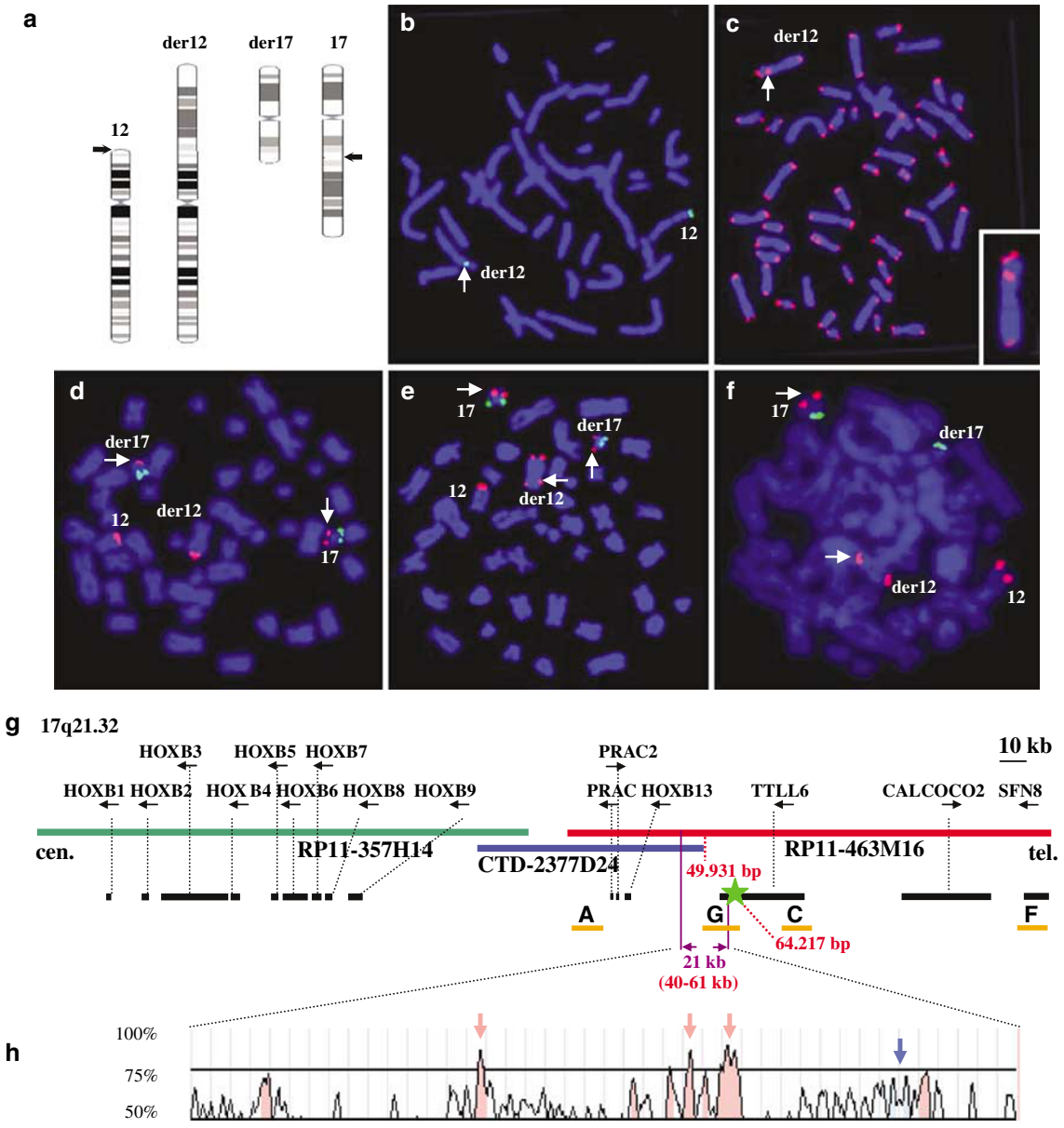

Figure 2 Cytogenetic and molecular characterization of the t(12;17)(p13.3;q21.3) translocation. (**a**) Ideograms of the patient's normal and derivative chromosomes 12 and 17. The breakpoints predicted by G-band analysis are indicated by arrows. (**b**) Hybridization of a 12p subtelomeric probe (8M16/SP6, Vysis) to the normal 12 and the der(12) (arrow). (**c**) Hybridization with telomeric hexamer repeats revealed an interstial telomere (arrow) on the der(12) (inset). (**d**–**f**) High-resolution FISH mapping of BAC/PACs and BAC subfragments to patient's metaphase spreads. PACs CTC-221K18 (labeled by Cy3 in red) and 202I17 (labeled by FITC in green) from the 12q and 17p subtelomeres were used for chromosome identification. PAC CTD-2377D24 (**d**, red signals indicated by arrows) produced signals on the normal 17 and the der(17), proximal to the breakpoint. BAC RP11-463M16 (**e**, red signals indicated by arrows) hybridized to the normal 17 and both derivative chromosomes and, thus, contains the 17q21.3 breakpoint. PCR fragment 463M16G (**f**, red signals indicated by arrows) hybridized to the normal 17 and the der(12), distal to the breakpoint. (**g**) Chromosome 17q21.32 breakpoint contig of clones RP11-357H14 (green bar), CTD-2377D24 (blue bar), and RP11-463M16 (red bar). The distal end of the breakpoint-flanking (by FISH) PAC CTD-2377D24 corresponds to basepair 49 931 of the breakpoint-spanning BAC RP11-463M16 (vertical red dotted line). Smaller black bars below the BAC contig indicate the location of genes in the breakpoint region. Arrows below the corresponding gene names (above the BAC contig) indicate the direction of transcription. Green star indicates the *TTLL6* stop codon outside the breakpoint region. Small orange bars below the BAC contig indicate the location of long-range PCR products used for FISH mapping. The breakpoint-containing interval (corresponding to the region from 40 to 61 kb of BAC RP11-463M16) is indicated by horizontal purple arrows. (**h**) VISTA conservation plot of the enlarged breakpoint interval (window size 50 bp, homology threshold 75%). Conserved non-genic sequences between humans and mouse are represented as pink peaks; conserved genic sequences are light blue. The distal blue peak (indicated by a blue arrow) corresponds to the 3′ UTR of *TTLL6*.

indicated by arrows), C, and F all hybridized to the normal 17 and the der(12), which would be consistent with a location distal to the breakpoint. Because PAC CTD-2377D24 and BAC fragment 463M16G did not produce split hybridization signals, but hybridized to different derivative chromosomes, the 17q21.3 breakpoint must be contained in the very distal part (<10 kb) of PAC CTD-2377D24, the proximal part (<10 kb) of BAC fragment 463M16G, or the small interval (1090 bp) between these two DNA segments. In our experience, 10 kb of genomic DNA sequence is more than sufficient to generate a detectable FISH signal at the target region. Collectively, our FISH mapping results narrowed the breakpoint down to a 21-kb interval from 40 to 61 kb of the breakpoint-spanning BAC RP11-463M16 (Figure 2g, indicated by horizontal purple arrows).

Genes near the 17q21.3 breakpoint region

The breakpoint-spanning clone RP11-463M16 contains six validated genes (Figure 2g; Table 3). The coding sequence of tubulin tyrosine ligase-like family, member 6 (*TTLL6*), a gene of unknown function, lies distal to the breakpoint region. The stop codon of *TTLL6* (Figure 2g, green star) corresponds to basepair 64 217 of RP11-463M16, implying that only the 3′ UTR lies within the distal breakpoint region (Figure 2h, indicated by vertical blue arrow). Interestingly, the transcription factor *HOXB13* lies in close proximity (<30 kb) at the proximal side of the breakpoint on the der(17). The *HOXB* gene cluster on chromosome 17q21.3 contains *HOXB1* to *HOXB9* and *HOXB13*, which is approximately 100 kb upstream of *HOXB9* (Figure 2g). All 10 *HOXB* genes are transcribed in the same direction with the 5′ end toward *HOXB13* and the 3′ end toward *HOXB1*.

Because the patient's phenotype, including hexadactyly and other skeletal abnormalities, is consistent with misregulation of a *HOXB* gene(s), we conclude that the 17q21.3 rearrangement separated the *HOXB* gene cluster from control elements and/or changed its local chromatin environment. Comparison of human and mouse genomic sequences with the GenomeVISTA program revealed three conserved non-genic segments of >50 bp with >75% sequence similarity in the 21-kb breakpoint interval (from 40 to 61 kb of BAC RP11-49931) at the 5′ region of the *HOXB* cluster (Figure 2h, indicated by vertical pink arrows). These evolutionarily highly conserved segments may be good candidates for *cis*-regulatory elements. Considering that the 17q21.3 breakpoint acquired telomeric hexamer repeats, the 5′ region of the *HOXB* gene cluster on the der(17) was fused to a repetitive DNA domain, which may have changed its higher-order chromatin structure and/or nuclear localization. Mammalian telomeres are located in specific cell-cycle-dependent areas of the nucleus.[19] In yeast it was shown that the transcriptional states of telomeric genes depend on spatial positioning in transcription-compentent *versus* transcription-incompetent nuclear compartments.[20]

To provide additional evidence for a possible position effect, the expression of *HOXB3*, *HOXB4*, *HOXB8*, *HOXB9*, *HOXB13*, *TTLL6*, *CALCOCO2*, and *SNF8* was analyzed by standard RT-PCR (using 40 ng cDNA) in lymphoblastoid cell lines of the patient and 10 normal control individuals. Unfortunately, *HOXB8*, which is likely to play a role in limb development,[21] as well as the breakpoint-flanking genes *HOXB13* and *TTLL6,* were not or only very lowly expressed in lymphoblasts. When using increased amounts (200 ng) of cDNA in the PCR, low *HOXB8*, *HOXB13*, and *TTLL6* transcript levels were detected in some of the tested cell lines. However, repeated experiments using the same cDNA samples under identical conditions as well as experiments with different cDNA preparations from the same cell lines suggested that RT-PCR amplification occurred in a more or less stochastic manner. Therefore, these genes were excluded from further expression analyses. In contrast, *HOXB3* and *HOXB4*, which are more 3′ in the *HOXB* cluster, and *HOXB9*, which is relatively 5′, as well as *CALCOCO2* and *SFN8* from the distal breakpoint region, were expressed at quantifiable levels in lymphoblastoid cell lines. Transcripts were easily amplified by standard RT-PCR from lymphoblasts of the patient and all 10 control individuals. However, quantitative real-time PCR demonstrated that expression of all five tested genes varied considerably (by a factor of 5–10) between cell lines (data not shown). We therefore conclude that EBV transformation and/or prolonged cell culture caused aberrant/ectopic expression of these genes and that RT-PCR data from

Table 3 Genes in the breakpoint region

Name	*Gene description*	*Expression and/or function*
PRAC	Prostate/rectum and colon protein	Expressed in prostate, rectum, and distal colon; regulatory role in nucleus
PRAC2	Prostate/rectum and colon protein 2	Possible function in prostate growth and development
HOXB13	Homeobox B13	Transcription factor belonging to homeobox gene family
TTLL6	Tubulin tyrosine ligase-like family, member 6	Tubulin-tyrosine ligase activity
CALCOCO2	Calcium binding and coil–coil domain 2	Subunit of nuclear domain 10 (ND10) bodies; role in viral life cycle
SFN8	ESCRT-II complex subunit, homolog (*Saccharomyces cerevisiae*)	Protein sorting, multivesicular body vesicle formation

lymphoblastoid cells do not allow any conclusion as to their quantitative expression in affected tissues. For *HOXB9*, *CALCOCO2*, and *SNF8*, we identified transcribed SNPs in our patient. Sequencing of RT-PCR products revealed biallelic expression of these genes in the patient's lymphoblasts.

Discussion

HOX genes are crucial for positioning organs along the anterior–posterior axis of the developing vertebrate embryo.[22,23] In the human genome, 39 *HOX* genes belonging to 13 paralogous groups are arranged in four clusters on chromosomes 7p15.3 (*HOXA*), 17q21.3 (*HOXB*), 12q13.3 (*HOXC*) and 2q31 (*HOXD*).[24] Gene expression within each cluster follows the so-called 'colinearity rule'. This means that *HOX* genes in the 3′ region of a cluster are activated first and in anterior areas of the embryo, whereas genes in the 5′ region are transcribed later and in more caudal areas.[22] In certain tissues, *HOX* genes also display 'quantitative colinearity'. The gene at the 5′ end shows the highest expression level and the more 3′ located genes are expressed at progressively lower levels.[25] Real-time PCR analysis of the 39 human *HOX* genes in normal adult organs revealed that 5′ located *HOX* genes are expressed preferentially in organs of the caudal body parts. In general, the expression patterns of neighboring *HOX* genes in the same cluster are more similar to each other than to their paralogs in other clusters.[16]

Natural mutants of mammalian *Hox* genes are rare. Hypodactyly mice result from a deletion within the *Hoxa13* locus.[26] The different functions of individual members of the *Hoxb* gene cluster have been extensively studied in knockout mice. *Hoxb1*, *Hoxb2*, and *Hoxb3* are involved in hindbrain specification.[27–29] *Hoxb2* and *Hoxb4* are important for sternum development.[28,30] *Hoxb3* and *Hoxb4* play roles in hematopoietic stem cell regeneration and proliferative response.[31] *Hoxb5* is necessary for differentiation of angioblasts and mature endothelial cells from their mesoderm-derived precursors.[32] *Hoxb6* controls generation, proliferation, and/or survival of erythroid progenitor cells.[33] *Hoxb7* knockout mice have fused ribs in the upper thoracic region.[34] *Hoxb8* knockouts show abnormal grooming behavior and central nervous system abnormalities,[35] whereas ectopic expression of *Hoxb8* results in a mirror-image duplication in the forelimb.[21] *Hoxb9* together with its paralogs *Hoxa9* and *Hoxd9* controls development of the mammary gland in pregnancy.[36] *Hoxb13* knockouts display an overgrowth of all major structures derived from the tail bud, including the secondary neural tube, the caudal spinal ganglia, and vertebrae, implying that *Hoxb13* may function as an inhibitor of neuronal cell proliferation, an activator of apoptotic pathways in the neural tube, and a general repressor of growth in the caudal vertebrae.[37] *Hoxb13* is also required for normal differentiation and secretory function of the ventral prostate.[38] Targeted deletion within the mouse *Hoxb* cluster from *Hoxb1* to *Hoxb9* resulted in a series of single segment anterior homeotic transformations along the cervical and thoracic vertebral column and defects in sternum morphogenesis.[39] Interestingly, *Hoxb13* expression was not affected by *Hox1–Hox9* deletion, suggesting that its regulatory element(s) is located 5′ to *Hoxb9*. However, so far there is no evidence from animal models implicating a *HOXB* gene(s) in postaxial hexadactyly, which is the most specific symptom of our patient.

In humans, several genetic disorders of the skeletal system are due to mutations in different *HOX* genes. Single basepair deletions in *HOXA11* cause amegakaryocytic thrombocytopenia and radioulnar synostosis.[40] Heterozygous mutations in *HOXA13* are associated with hand–foot–genital syndrome and the closely related Guttmacher syndrome.[41,42] A missense mutation in *HOXD10* segregates in a family with rocker-bottom feet and Charcot-Marie-Tooth disease.[43] Polyalanine coding repeat expansions in exon 1 of *HOXD13* cause synpolydactyly.[44,45] Intragenic frameshift deletions,[46] missense mutations in exon 2[47,48] and an acceptor splice site mutation[49] have been associated with novel hand and/or foot malformations. It is important to note that breakpoints in chromosome 2q31 near the *HOXD* cluster were found in four independent patients with balanced chromosome rearrangements and various limb and skeletal malformations.[11,12] Similar to our case, these disease-associated chromosome rearrangements did not disrupt a gene(s) but most likely exerted position effects by disturbing normal *HOXD* gene expression. Interactions between regulatory elements at the 5′ border of the *Hoxd* cluster and the digit enhancer that lies at least 100 kb 5′ to the *Hoxd* gene cluster appear to be crucial for establishing quantitative colinearity in the mouse *Hoxd* cluster.[50]

To our knowledge, the patient described here represents the first example of a disease-associated translocation breakpoint near the *HOXB* cluster. Circumstantial evidence suggests that misregulation of a *HOXB* gene(s) by position effect is responsible for the patient's phenotype. Mouse *Hoxb* genes are known to play important functions in skeletal and central nervous system development. The *HOXB* cluster lies within 30 kb of the breakpoint on the patient's chromosome 17q21.3 and was moved from a euchromatic chromatin environment in close proximity of a repetitive chromatin domain (telomeric hexamer repeats). The breakpoint region at the 5′ end of the *HOXB* cluster contains evolutionarily conserved non-genic sequences that may act as cis-acting DNA elements. Unfortunately, expression analyses are limited with human patients. In our patient with mental retardation and limb and rib malformations, it was not possible to study gene expression in the relevant cell types/tissues. It is well known that *HOX* and other developmental control genes

show tissue-specific expression patterns.[51,52] The observed differences between established lymphoblastoid cell lines of the patient and normal control individuals appear to be secondary to the genetic condition of the donors. Nevertheless, it is plausible to assume that the translocation breakpoint near the 5′ end of the *HOXB* cluster interferes with the colinear expression pattern of *HOXB* genes in organs that are affected in our patient. Separation of mouse *Hox* genes from regulatory sequences located at a distance outside the cluster is known to cause misexpression.[53,54] Because both *HOXB13*[55,56] and the *PRAC* genes[56,57] in the breakpoint region have been implicated in human prostate cancer, the patient will be followed for this. The described t(12;17) translocation patient provides a promising starting point for the identification and characterization of regulatory elements of the *HOXB* cluster. Indeed, alterations of *HOX* genes may be an underestimated cause for human genetic disease.

Acknowledgements

We thank Karen Stout, Eva Weis, and Cornelia Wetzig for excellent technical assistance and Dr Nicolai Kohlschmidt for helpful discussion.

Electronic-Database Information

GenomeVISTA program (http://www-gsd.lbl.gov/vista/)
PubMed (http://www.ncbi.nlm.nih.gov/entrez/)
Wellcome Trust Sanger Institute Ensembl contigs (http://www.ensembl.org).

References

1 Kleinjan DK, van Heyningen V: Long-range control of gene expression: emerging mechanisms and disruption in disease. *Am J Hum Genet* 2005; **76**: 8–32.
2 De Kok YJM, Vosenaar ER, Cremers CW *et al*: Identification of a hot spot for microdeletions in patients with X-linked deafness type 3 (DFN3) 900 kb proximal to the DFN3 gene *POU3F4*. *Hum Mol Genet* 1996; **5**: 1229–1235.
3 Belloni E, Muenke M, Roessler E *et al*: Identification of *Sonic hedgehog* as a candidate gene responsible for holoprosencephaly. *Nat Genet* 1996; **14**: 353–356.
4 Velagaleti GVN, Bien-Willner GA, Northup JK *et al*: Position effects due to chromosome breakpoints that map ~900 kb upstream and 1.3 Mb downstream of *SOX9* in two patients with campomelic dysplasia. *Am J Hum Genet* 2005; **76**: 652–662.
5 Fantes J, Ragge NK, Lynch SA *et al*: Mutations in *SOX2* cause anophthalmia. *Nat Genet* 2003; **33**: 461–463.
6 Warburton D: *De novo* balanced chromosome rearrangements and extra marker chromosomes identified at prenatal diagnosis: clinical significance and distribution of breakpoints. *Am J Hum Genet* 1991; **49**: 995–1001.
7 Abeysinghe SS, Stenson PD, Krawczak M, Cooper DN: Gross rearrangement breakpoint database (GRaBD). *Hum Mutat* 2004; **23**: 219–221.
8 Bugge M, Bruun-Petersen G, Brøndum-Nielsen K *et al*: Disease associated balanced chromosome rearrangements: a resource for large scale genotype–phenotype delineation in man. *J Med Genet* 2000; **37**: 858–865.
9 Goodman FR: Limb malformations and the human *HOX* genes. *Am J Med Genet* 2002; **112**: 256–265.
10 Kornak U, Mundlos S: Genetic disorders of the skeleton: a developmental approach. *Am J Hum Genet* 2003; **73**: 447–474.
11 Spitz F, Montavon T, Monso-Hinard C *et al*: A t(2;8) balanced translocation with breakpoints near the human *HOXD* complex causes mesomelic dysplasia and vertebral defects. *Genomics* 2002; **79**: 493–498.
12 Dlugaszewska B, Silahtaroglu A, Menzel C *et al*: Breakpoints around the *HOXD* cluster result in various limb malformations. *J Med Genet* 2005; **43**: 111–118.
13 Yue Y, Grossmann B, Holder SE, Haaf T: *De novo* t (7;10) (q33;q23) translocation and closely juxtaposed microdeletion in a patient with macrocephaly and developmental delay. *Hum Genet* 2005; **117**: 1–8.
14 Yue Y, Stout K, Grossmann B *et al*: Disruption of *TCBA1* associated with a *de novo* t(1;6)(q32.2;q22) presenting in a child with developmental delay and recurrent infections. *J Med Genet* 2006; **43**: 409–412.
15 Wirth J, Nothwang HG, van der Maarel S *et al*: Systematic characterisation of disease associated balanced chromosome rearrangements by FISH: cytogenetically and genetically anchored YACs identify microdeletions and candidate regions for mental retardation genes. *J Med Genet* 1999; **36**: 271–278.
16 Takahashi Y, Hamada JI, Murakawa K *et al*: Expression profiles of 39 *HOX* genes in normal human adult organs and anaplastic thyroid cancer cell lines by quantitative real-time RT-PCR system. *Exp Cell Res* 2004; **293**: 144–153.
17 Lin Y, Waldman AS: Capture of DNA sequences at double-strand breaks in mammalian chromosomes. *Genetics* 2001; **158**: 1665–1674.
18 Nergadze SG, Rocchi M, Azzalin CM, Mondello C, Giulotto E: Insertion of telomeric repeats at intrachromosomal break sites during primate evolution. *Genome Res* 2004; **14**: 1704–1710.
19 Vourc'h C, Taruscio D, Boyle AL, Ward DC: Cell cycle-dependent distribution of telomeres, centromeres, and chromosome-specific subsatellite domains in the interphase nucleus of mouse lymphocytes. *Exp Cell Res* 1993; **205**: 142–151.
20 Feuerbach F, Galy V, Trelles-Sticken E *et al*: Nuclear architecture and spatial positioning help establish transcriptional states of telomeres in yeast. *Nat Cell Biol* 2002; **4**: 212–214.
21 Charite J, de Graaff W, Shen S, Deschamps J: Ectopic expression of *Hoxb-8* causes duplication of the ZPA in the forelimb and homeotic transformation of axial structures. *Cell* 1994; **78**: 589–601.
22 Krumlauf R: *Hox* genes in vertebrate development. *Cell* 1994; **78**: 191–201.
23 Duboule D: Vertebrate *Hox* genes and proliferation: an alternative pathway to homeosis? *Curr Opin Genet Dev* 1995; **5**: 525–528.
24 Apiou F, Flagiello D, Cillo C, Malfoy B, Poupon MF, Dutrillaux B: Fine mapping of human *HOX* gene clusters. *Cytogenet Cell Genet* 1996; **73**: 114–115.
25 Dolle P, Izpisua-Belmonte JC, Brown JM, Tickle C, Duboule D: *HOX-4* genes and the morphogenesis of mammalian genitalia. *Genes Dev* 1991; **5**: 1767–1777.
26 Mortlock DP, Post LC, Innis JW: The molecular basis of hypodactyly (Hd): a deletion in *Hoxa13* leads to arrest of digital arch formation. *Nat Genet* 1996; **13**: 284–289.
27 Studer M, Lumsden A, Ariza-McNaughton L, Bradley A, Krumlauf R: Altered segmental identity and abnormal migration of motor neurons in mice lacking *Hoxb-1*. *Nature* 1996; **384**: 630–634.
28 Barrow JR, Capecchi MR: Targeted disruption of the *Hoxb-2* locus in mice interferred with expression of *Hoxb-1* and *Hoxb-4*. *Development* 1996; **122**: 3817–3828.
29 Manley NR, Capecchi MR: *Hox* group 3 paralogous genes act synergistically in the formation of somatic and neural crest-derived structures. *Dev Biol* 1997; **192**: 274–288.
30 Ramirez-Solis R, Zheng H, Whiting J, Krumlauf R, Bradley A: *Hoxb-4* (*Hox-2.6*) mutant mice show homeotic transformation of a cervical vertebra and defects in the closure of the sternal rudiments. *Cell* 1993; **73**: 279–294.

31 Björnsson JM, Larsson N, Brun AC *et al*: Reduced proliferative capacity of hematopoietic stem cells deficient in *Hoxb3* and *Hoxb4*. *Mol Cell Biol* 2003; **23**: 3872–3883.
32 Wu Y, Moser M, Bautch VL, Patterson C: *HoxB5* is an upstream transcriptional switch for differentiation of the vascular endothelium from precursor cells. *Mol Cell Biol* 2003; **23**: 5680–5691.
33 Kappen C: Disruption of the homeobox gene *Hoxb-6* in mice results in increased numbers of early erythrocyte progenitor. *Am J Hematol* 2000; **65**: 111–118.
34 Chen F, Greer J, Capecchi MR: Analysis of *Hoxa7/Hoxb7* mutants suggests periodicity in the generation of the different sets of vertebrae. *Mech Develop* 1998; **77**: 49–57.
35 Greer JM, Capecchi MR: *Hoxb8* is required for normal grooming behavior in mice. *Neuron* 2002; **33**: 23–34.
36 Chen F, Capecchi MR: Paralogous mouse *Hox* genes, *Hoxa9*, *Hoxb9*, and *Hoxd9*, function together to control development of the mammary gland in response to pregnancy. *Proc Natl Acad Sci USA* 1999; **96**: 541–546.
37 Economides KD, Zeltser L, Capecchi MR: *Hoxb13* mutations cause overgrowth of caudal spinal cord and tail vertebrae. *Dev Biol* 2003; **256**: 317–330.
38 Economides KD, Capecchi MR: *Hoxb13* is required for normal differentiation and secretory function of the ventral prostate. *Development* 2003; **130**: 2061–2069.
39 Medina-Martinez O, Bradley A, Ramirez-Solis R: A large targeted deletion of *Hoxb1-Hoxb9* produces a series of single-segment anterior homeotic transformations. *Dev Biol* 2000; **222**: 71–83.
40 Thompson AA, Nguyen LT: Amegakaryocytic thrombocytopenia and radio-ulnar synostosis are associated with *HOXA11* mutation. *Nat Genet* 2000; **26**: 397–398.
41 Mortlock DP, Innis JW: Mutations of *HOXA13* in hand–foot–genital syndrome. *Nat Genet* 1997; **15**: 179–180.
42 Innis JW, Goodman FR, Bachelli C *et al*: A *HOXA13* allele with a missense mutation in the homeobox and a dinucleotide deletion in the promoter underlies Guttmacher syndrome. *Hum Mut* 2002; **19**: 573–574.
43 Shrimpton AE, Levinson EM, Yozawitz JM *et al*: A *HOX* gene mutation in a family with isolated congenital vertical talus and Charcot-Marie-Tooth disease. *Am J Hum Genet* 2004; **75**: 92–96.
44 Muragaki Y, Mundlos S, Upton J, Olsen BR: Altered growth and branching patterns in synpolydactyly caused by mutations in *HOXD13*. *Science* 1996; **272**: 548–551.
45 Akarasu AN, Stoilov I, Yilmaz E, Sayli BS, Sarfarazi M: Genomic structure of *HOXD13* gene: a nine polyalanine duplication causes synpolydactyly in two unrelated families. *Hum Mol Genet* 1996; **5**: 945–952.
46 Goodman FR, Giovannucci-Uzielli ML, Hall C, Reardon W, Winter RM, Scambler PJ: Deletions in *HOXD13* segregate with an identical, novel foot malformation in two unrelated families. *Am J Hum Genet* 1998; **63**: 992–1000.
47 Debeer P, Bacchelli C, Scambler PJ, De Smet L, Fryns JP, Goodman FR: Severe digital abnormalities in a patient heterozygous for both a novel missense mutation in *HOXD13* and a polyalanine expansion in *HOXA13*. *J Med Genet* 2002; **39**: 852–856.
48 Caronia G, Goodman FR, McKeown CM, Scambler PJ, Zappavigna V: An I47L substitution in the *HOXD13* homeodomain causes a novel limb malformation by producing a selective loss of function. *Development* 2003; **130**: 1701–1712.
49 Kan SH, Johnson D, Giele H, Wilkie AO: An acceptor splice site mutation in *HOXD13* results in variable hand, but consistent foot malformations. *Am J Med Genet* 2003; **121A**: 69–74.
50 Kmita M, Fraudeau N, Herault Y, Duboule D: Serial deletions and duplications suggest a mechanism for the colinearity of *Hoxd* genes in limbs. *Nature* 2002; **420**: 145–150.
51 Shen WF, Largman C, Lowney P *et al*: Lineage-restricted expression of homeobox-containing genes in human hematopoietic cell lines. *Proc Natl Acad Sci USA* 1989; **86**: 8536–8540.
52 Fuller JF, McAdara J, Yaron Y, Sakaguchi M, Fraser JK, Gasson JC: Characterization of *HOX* gene expression during myelopoiesis: role of *HOX A5* in lineage commitment and maturation. *Blood* 1999; **93**: 3391–3400.
53 Herault Y, Beckers J, Gerard M, Duboule D: *Hox* gene expression in limbs: colinearity by opposite regulatory controls. *Dev Biol* 1999; **208**: 157–165.
54 Spitz F, Gonzalez F, Peichel C, Vogt TF, Duboule D, Zakany J: Large scale transgenic and cluster deletion analysis of the *HoxD* complex separate an ancestral regulatory module from evolutionary innovations. *Genes Dev* 2001; **15**: 2209–2214.
55 Jung C, Kim RS, Zhang HJ, Lee SJ, Jeng MH: *HOXB13* induces growth suppression of prostate cancer cells as a repressor of hormone-activated androgen receptor signalling. *Cancer Res* 2004; **64**: 9185–9192.
56 Edwards S, Campell C, Flohr P *et al*: Expression analysis onto microarrays of randomly selected cDNA clones highlights *HOXB13* as a marker of human prostate cancer. *Br J Cancer* 2005; **92**: 376–381.
57 Olsson P, Motegi A, Bera TK, Lee B, Pastan I: *PRAC2*: a new gene expressed in human prostate and prostate cancer. *Prostate* 2003; **56**: 123–130.